The Journal of Chemical Physics

An experimental investigation of periodic and chaotic electrochemical oscillations in the anodic dissolution of copper in phosphoric acid

F. N. Albahadily and Mark Schell

Citation: J. Chem. Phys. 88, 4312 (1988); doi: 10.1063/1.453790
View online: http://dx.doi.org/10.1063/1.453790
View Table of Contents: http://jcp.aip.org/resource/1/JCPSA6/v88/i7
Published by the American Institute of Physics.

An experimental investigation of periodic and chaotic electrochemical oscillations in the anodic dissolution of copper in phosphoric acid

F. N. Albahadily and Mark Schell
Department of Chemistry, Southern Methodist University, Dallas, Texas 75275

(Received 5 November 1987; accepted 17 December 1987)

The response of the current to an applied potential was monitored in an open electrochemical system consisting of a rotating copper disk as the working electrode, a calomel reference electrode, and a platinum counter electrode, all of which were in contact with a solution of 85% phosphoric acid. In addition to stable stationary states, the applied potential induced oscillatory states which were either periodic or chaotic. Transitions from a stationary state to sustained oscillations were found to take place either through a Hopf bifurcation or by way of a mechanism that gives rise to states possessing complex combinations of small and large amplitude oscillations (mixed-mode oscillations). Within the parameter ranges for which sustained oscillations occurred, we discovered sequences of period doubling bifurcations. Aperiodic oscillations were observed just beyond the limit at which a sequence terminated. Phase trajectories were constructed from time-series data for these aperiodic states from which we produced one-humped, one-dimensional maps. A trajectory was also constructed that closely resembled a homoclinic orbit. Mixed-mode oscillations were found which have the same properties as those previously observed in the Belousov–Zhabotinskii reaction. The production of copper was observed in this electrochemical system which suggests that the reaction of disproportionality may be part of a feedback mechanism that is responsible for the complex dynamical behavior.

I. INTRODUCTION

Sustained oscillations have been observed in the current and voltage of a large number of electrochemical systems and under a wide variety of conditions.[1–5] The theoretical description of these oscillations[6–10] combined with experimental studies have increased our knowledge of processes that occur on or near electrodes. Most investigations have focused on the cause of electrochemical oscillations. Little attention has been paid to the nature of the transition from stable-steady-state behavior to sustained oscillations and on the possible bifurcations between different types of oscillatory behavior.[3]

In this paper we report the results of an experimental study on the anodic dissolution of copper in phosphoric acid[11,12] using a rotating copper disk as the working electrode.[4] The purpose of this work is to examine whether the oscillations that have been observed in the copper–phosphoric acid system consist of different dynamical behaviors and, if this is the case, to determine whether the different oscillatory states and bifurcations to these states can be characterized. Such characterizations will serve as tests for theories of electrochemical processes and the approximations they invoke. The techniques we use are the same as those from nonlinear dynamics that have been applied to complex chemical reactions.[13–17]

A summary of current understanding of the processes that accompany the oxidation of copper at a rotating disk in phosphoric acid is contained in Ref. 4. All relevant electrochemical reactions occur in a thin boundary layer adjacent to the surface of the copper disk. Little can be stated with certainty in regards to these reactions since a qualitative analysis of the chemical composition in the boundary layer has not yet been accomplished. Partially soluble oxide and phosphate films that inhibit the processes by which copper is dissolved have been proposed and the formation and dissolution of such a film has been considered to play an important role in the onset of oscillatory instabilities. However, the formation of a solid film rather than a highly viscous boundary layer has not been proved. Using impedance measurements, Glarum and Marshal[4(b)] have provided evidence that a negatively charged surface layer develops at the rotating copper disk. The structure of the layer depends on the potential of the working electrode and can grow as large as 100 Å. These authors also showed that the dissolution process is coupled in complicated ways to the hydrodynamic processes. For example, the dependence of the limiting current on viscosity was found to be different than that predicted by the Levich equation.[4(a)] It is hoped that our initial study presented in the present paper will lead to the development of techniques that combines nonlinear dynamics with the methods of electrochemistry for the purpose of obtaining information on mechanisms of complicated electrochemical processes such as the dissolution of copper.

All measurements reported in this paper were obtained by monitoring the response of the current to a potential that was applied with a potentiostat. In Sec. II of this paper we describe the apparatus and procedures employed in the experiments.

A diagram is presented in Sec. III that contains measured boundaries in the parameter plane, rotation rate vs the potential set at the working electrode, which separate the conditions for which sustained oscillations were observed from those for which only steady states were found. An analysis of time series for the current is also presented for the purpose of characterizing the oscillatory behavior in the vicinity of the measured boundaries. A large portion of the

 0021-9606/88/074312-08$02.10

boundaries consists of points at which the system was observed to make a transition from a stable steady state to small-amplitude, harmonic-like oscillations. At points on the remaining portion of the measured boundaries, transitions to oscillations gave rise to states which possessed both large and small amplitude oscillations (mixed-mode oscillations). From experimental data collected in the vicinity of this latter behavior, we used the time-delay method[13–15] to construct a curve that nearly duplicates the properties of a homoclinic orbit that satisfies the conditions of Sil'nikov's theorem.[18,19]

Within the region of parameter space at which sustained oscillations occurred we found a variety of dynamical behavior that possesses many of the features of the behavior observed in several experimental investigations on complex chemical reactions.[13–17] When the potential of the working electrode was slowly varied at specific rotation rates, a sequence of period doubling bifurcations took place.[20] Beyond the point at which a sequence terminated, the response to the potential consisted of chaotic oscillations.[20] For several other ranges of parameters we measured waveforms of mixed-mode oscillations that are not a continuation of those found near stable steady states. The results and analysis of measurements on these various behaviors are presented in Sec. IV.

An additional observation is presented in Sec. V that implies that copper is formed through a chemical reaction which, in turn, contradicts many of the proposed electrokinetic mechanisms for the dissolution of copper in phosphoric acid. We conclude this section with a discussion of our results.

II. EXPERIMENTAL

A schematic of the cell and the configuration for the electrodes used in the experiments is shown in Fig. 1. A rotating disk, total diameter 12.5 mm, 5 mm diameter in copper, insulated with Teflon and attached to a PAR model 616 rotator, served as the working electrode [see Ref. 21(a) for a description of the theory and applications of a rotating disk electrode]. The copper was purchased from Alfa Products (Danvers, Massachusetts) in the form of rods, 9.5 mm diameter, purity $>99\%$. A saturated calomel reference electrode (Sargent–Welch standard size) was positioned 1.5 cm from the working electrode with 0.5 cm of its end immersed in solution. The counter electrode, a strip of platinum, was located in a compartment that was connected through channels to the compartment of the two other electrodes, Fig. 1. Two compartments were used so that gas bubbles given off at the counter electrode would not be trapped at the surface of the rotating disk. The upper channel, see Fig. 1, ensures the prevention of a pressure gradient and is fitted with a frit so that solution is not circulated back into the left compartment under conditions in which the solution reaches the level of that channel (such conditions were avoided in taking the measurements presented in this paper). A solution of 85% phosphoric acid, reagent grade (J. T. Baker Chemical Co.) flowed through the cell with a flowrate of 3 ml/min. The input was located in the compartment containing the counter electrode, and the output was located in the other compartment. A volume of 50 ml was maintained in the compartment containing the working electrode.

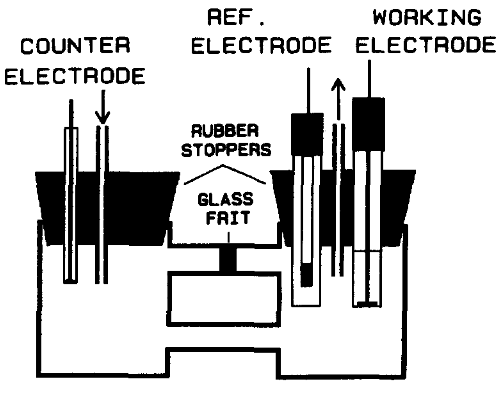

FIG. 1. Schematic of the electrochemical cell.

Applications of potentials to the cell and measurements of the current were made using a PAR 273, which was interfaced with an IBM XT computer for the purpose of acquiring and analyzing data. The current was also recorded on a strip chart and an x,y recorder. Henceforth, all values for potentials reported in this paper are those set for the working electrode by the potentiostat.

The cell, Fig. 1, was thermostated at various temperatures. Only results for the temperatures -17.5 and -24.5 °C are reported in this paper. At high temperatures, the period of oscillation is too short (<0.05 s at 50.0 °C) for our recorders to capture the full character of the waveforms.

The cell was saturated with nitrogen during several experiments. However, this procedure was discontinued after we found that it caused no observable difference in the measurements.

Before each set of experiments, the working electrode was smoothed with 600 mesh sandpaper and the system was moved through the electropolishing region[4,11,12] four or five times with a sweep rate of 10 mV/s. At the low temperatures that were used, the average measured current was approximately -1.0 mA for values of the potential that were of interest. Consequently, experiments could be carried out for three to four hours before the disk electrode required resanding. Experiments were halted after deformations in the copper surface or the formation of a bubble on the disk were observed.

Finally, we point out that it is only the experimental analog of "asymptotic behavior" that is discussed in this paper. All measurements presented in Secs. III and IV were carried out either at fixed values of the constraints and after transients decayed or during the variation of a constraint. The variation was carried out slowly enough that the system would remain close to its "asymptotic state."

III. BIFURCATIONS FROM STABLE STATIONARY STATES TO SUSTAINED OSCILLATIONS AND ACCOMPANYING LOCAL BEHAVIOR

In this section we present measured boundaries that separate parameter space into two parts. The conditions in one part are such that sustained oscillations were observed, whereas those in the other part are such that the system was found to support only stationary states. The oscillatory behavior investigated at values of parameters in the vicinity of these boundaries is also described. We describe the various types of dynamical behavior that were detected for parameter values within the region for which sustained oscillations occurred, but outside the neighborhood of the boudaries, in Sec. IV.

A. Bifurcation boundaries in parameter space

We have constructed from measurements at a temperature of − 17.5 °C the boundaries, which separate the region for which asymptotic oscillatory states were observed from that for which only stable stationary states were found, in the parameter plane rotation rate of the working electrode vs the potential V, set for the working electrode. These boundaries are shown in Fig. 2. We note that a finite rotation rate is required for the working electrode in order to achieve sustained oscillations. The type of oscillatory behavior that was first encountered when moving the system into the region of parameter space for which sustained oscillations were found depended on the location that the boundary was crossed. Either small amplitude oscillations or a mixed combination of large and small amplitude oscillations (mixed-mode oscillations) were observed (see Fig. 2). We now discuss these two different types of behavior.

B. Hopf bifurication

When the system was moved across the solid portion of the boundary in Fig. 2 from a stationary state by slowly varying the potential or rotation rate, small amplitude, sinusoidal oscillations were first observed. The amplitude of oscillation became larger as the system was moved further into the region of sustained oscillations. These observations are consistent with the local behavior associated with an ordinary Hopf bifurcation (supercritical Hopf).[22] Although this bifurcation is simple and well understood, it has been observed in an isothermal reaction for the first time only recently.[23,24] A test for the occurrence of an ordinary Hopf bifurcation involves measuring the local dependence of the amplitude of oscillation on a bifurcation parameter. The results of one such set of measurements are shown in Fig. 3 where we have plotted the natural logarithm of the amplitude of oscillations as a function of the natural logarithm of the difference between the value of the potential V and its estimated value at the bifurcation point. A least squares fit is also shown which has a slope of 0.49; the theoretical value is 0.5.

C. Homoclinic orbits and transtions to mixed-mode oscillations

Large amplitude oscillations were observed when the system was moved from a steady state to a point within the region labeled SO and less than 1.0 mV from the dashed portion of the boundary in Fig. 2. In the neighborhood of the boundary points the large amplitude oscillations were mixed with small amplitude oscillations (see insert in Fig. 2). In most cases, close to the boundary points, both the number of sequential small amplitude oscillations and the time between two sequences appeared to behave as random quantities.

When we moved the system from the vicinity of a point on the dashed portion of the boundary further into the region of sustained oscillations by slowly decreasing the potential, several different periodic behaviors were observed, each still consisting of a mixture of both large and small amplitude oscillations. It was not possible to analyze the bifurcation structure along a line of decreasing potential as the parameter range for a particular stable state was very small. In

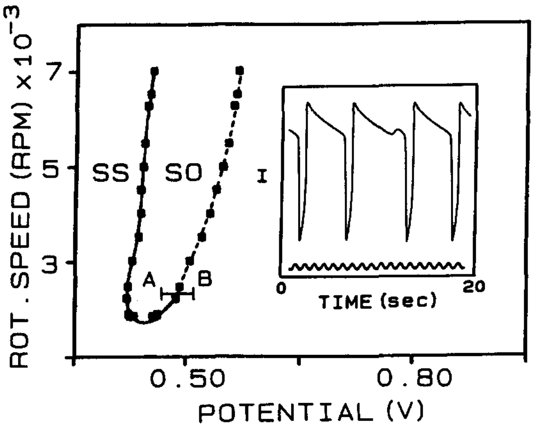

FIG. 2. Measured boundaries in the parameter plane, rotation speed vs the potential set for the working electrode, that separate the region for which sustained oscillations were observed (labeled SO) from the region for which only stable stationary states were found (labeled SS). Solid lines consist of points at which Hopf bifurcations occurred; dashed lines consist of points at which mixed-mode oscillations appeared. Temperature = − 17.5 °C. The small amplitude oscillations shown in the insert were observed just inside the solid portion of the boundary: rotation speed = 2200 rpm, potential = 427 mV, maximum absolute value of the current = 1.4 mA, minimum value = 1.2 mA. The waveform consisting of large and small amplitude oscillations was measured just inside the dashed portion of the boundary: rotation speed = 7000 rpm, potential = 567 mV, maximum absolute value of the current = 5.8 mA, minimum value = 1.4 mA. We describe in Sec II B the dynamical behavior observed when the system was moved along the line labeled A-B.

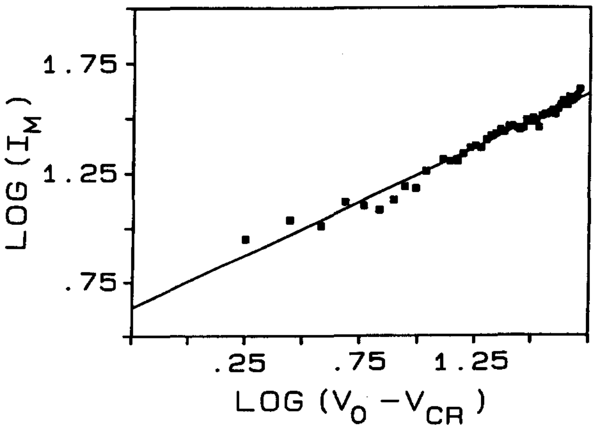

FIG. 3. Plot of the natural log of the amplitude of oscillation I_m (the maximum minus the minimum value of the current in units of mA) vs the natural log of the difference between the value of the potential V_0 set for the working electrode (in units of mV) and the critical value V_{CR}. Rotation speed = 1600 rpm; V_{CR} was estimated to be 426.0 mV. The solid curve is a least square fit which has a slope of 0.49.

fact, the whole set of mixed-mode oscillations would be completely missed in linear sweep voltammetry experiments[21(b)] that used sweep rates greater than 1 mV/s. Finally, periodic behavior was reached that consisted of only large amplitude oscillations. These large amplitude oscillations persisted for a relatively large range of values in the potential (at the rotation rate 4500 rpm only single peaked large amplitude oscillations were observed between 445 and 528 mV), whereas the range of values is small between the dashed portion of the boundary in Fig. 2 and the potential value at which only single peaked large amplitude oscillations first appeared (at the rotation rate 4500 rpm the range was less than 0.6 mV and this range decreased with respect to increases in rotation rate).

Transitions directly from stable, steady states to mixed-mode oscillations along an interval in parameter space without the presence of bistability (the coexistence of more than one stable state) is inconsistent with theory. (See Ref. 25 for theoretical descriptions of some examples of bifurcation structures that exist between stationary states and mixed-mode oscillations.) However, we were not able to observe bistability nor any state between mixed-mode oscillations and stable, steady states in the neighborhood of the dashed portion of the curve in Fig. 2. We believe that the bifurcation structure is too compressed to resolve in this part of the parameter plane.

The bifurcation structure was found to spread out at lower rotation rates. It is plausible that the structure along lines of constant rotation rate, which cross the dashed portion of the boundary, is the same as the structure observed in a traversal of the line A–B (see Fig. 2), except that the former is on a finer scale. Futhermore, we observed a phenomenon while moving the system along the path A–B, Fig. 2, that can account for the stated random behavior. Therefore, the changes in dynamical behavior that were detected when the system was moved along the path A–B are described in the remainder of this section.

At the lower potential end of the line, A–B, only single peaked large amplitude oscillations were observed. Upon increasing the potential, the system was moved through a set of mixed-mode oscillations. Measured waveforms for some of these oscillatory states are shown in Fig. 4. The average number of small amplitude oscillations increased with respect to increases in the potential until a value was reached where only periodic oscillations with the same small amplitude were observed. Moving further along the line A–B, the amplitude of the oscillations decreased until a Hopf bifurcation point was reached beyond which only stationary states were found.[26]

Both periodic and aperiodic mixed-mode oscillations were observed along the line A–B, Fig. 2. We now discuss results which imply that aperiodic oscillations which correspond to chaotic states can occur in this region of parameter space. Consider first the time series in Fig. 5(a) that was measured near the potential value at which the asymptotic behavior changed to small amplitude oscillations. The dashed line represents the value of the current measured at a stable stationary state for a value of the potential slightly greater than the value at which the Hopf bifurcation took place on the line A–B. To within a good approximation, the dashed line also represents the value of the current at the unstable stationary state for the value of the potential used to obtain the oscillations shown in Fig. 5(a), since the system was close to the Hopf bifurcation point (a difference of less than 1.5 mV exists between the potential value used in Fig. 5 and the value at the Hopf bifurcation point). Notice that

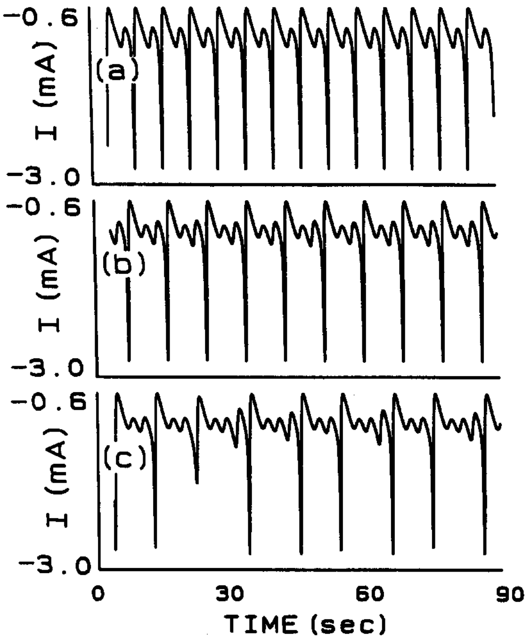

FIG. 4. Waveforms measured at different points along the curve labeled A–B in Fig. 2. Current I is plotted against time. Rotation speed = 2425 rpm, (a) $V_0 = 487.05$ mV; (b) $V_0 = 487.65$ mV; (c) $V_0 = 487.90$ mV.

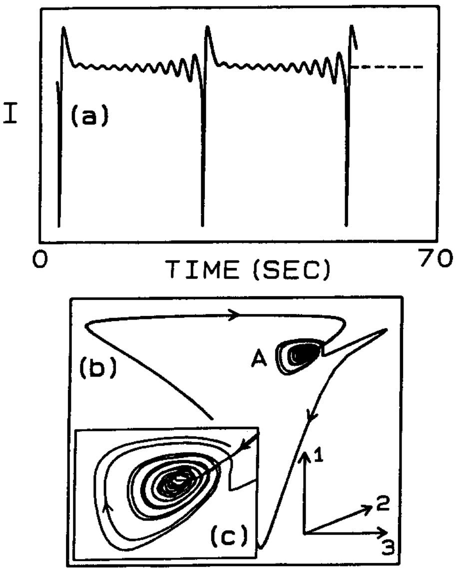

FIG. 5. (a) Measured current I plotted as a function time. Rotation speed = 2425 rpm, $V_0 = 488.05$ mV. Dashed curve represents the unstable-stationary-state value of the current. (b) Phase trajectory constructed from time series in (a). Axes are labeled: $1 = I(t + 2T)$, $2 = I(t)$, $3 = I(t + T)$; $T = 0.75$ s. (c) An enlargement of the surface [labeled A in (b)] on which the orbit spirals away from the fixed point (the position of the fixed point is at the center of the spirals).

after each large amplitude oscillation is completed in the time series, the current approaches its value at the unstable stationary state and then undergoes a sequence of small amplitude oscillations in which the amplitude slowly increases.

The dynamics associated with the time series in Fig. 5(a) can be more easily compared with a particular phenomenom of theoretical nonlinear dynamics if we examine a phase portrait constructed using the time-delay method.[13–15] Such a phase portrait, which is "embedded" in the space $[I(t), I(t+T), I(t+2T)]$, is shown in Figs. 5(b) and 5(c). Figure 5(c), an enlargement of the region labeled A in Fig. 5(b), shows an orbit that at some point in time is injected into a small neighborhood of the fixed point, the fixed point corresponds to the position of the unstable stationary state, and then spirals away on a two-dimensional surface. Note that each one of the spirals corresponds to a small amplitude oscillation. The orbit then appears to leave the surface (or drops over the apparent edge of the surface) but is eventually reinjected into a small neighborhood of the fixed point.

According to the theory of nonlinear dynamics,[25] an observation (like that given in the above) of an increase in the ratio of small to large amplitude oscillations is expected as the system approaches parameter values at which a homoclinic orbit exists, that is an orbit of inifinte period that begins and ends at the fixed point. Furthermore, nearly homoclinic conditions results in an orbit, such as the one in Fig. 5(c), which undergoes reinjections into a small neighborhood of the fixed point.[25] As a result of the location close to the Hopf bifurcation point for the conditions used in Fig. 5, the local relaxation towards the fixed point is faster than the local spiraling motion away from the fixed point. These properties satisfy Sil'nikov's theorem[18–19] and ensure the occurrence of chaotic states in neighboring parameter space.[25]

The changes that were observed in the dynamical behavior moving the system along the line A–B are qualitatively the same as those observed in moving the system along the lines of constant rotation rate that cross the dashed portion of the boundary (see Fig. 2). This is not surprising in that there should exist a continuation of the "surface" that contains the spirals in Fig. 5(c), into the surrounding parameter space. However, we did not find Hopf bifurcations nor only small amplitude oscillations along these lines in the neighborhood of the dashed portion of the boundary in Fig. 2. We suggest that this is due to a contraction of the bifurcation structure that increases with respect to increases in rotation rates. At high rotation rates (>6500 rpm) the mixed mode oscillations consist mainly of large amplitude oscillations with only the occassional appearance of small amplitude oscillations in the time series, see insert in Fig. 2, indicating that the surface containing the fixed point, which is a continuation of the surface containing the spirals in Fig. 5(c), is small. We speculate that this surface disappears at even higher rotation rates which would mean that the Hopf bifurcation is then replaced by another mechanism by which the stationary state loses its stability. At the present time we cannot test this idea since at these high rotation rates bubble formation on the disk is too frequent to allow experimental measurements.

IV. DYNAMICAL BEHAVIOR WITHIN THE REGION OF SUSTAINED OSCILLATIONS

We measured a wide variety of waveforms within the oscillatory region of Fig. 2 (labeled SO). The behaviors that were prevalent and simple to classify include sets of subharmonics and mixed-mode oscillations. These latter oscillations were not a continuation of the mixed-mode oscillations discussed in Sec. III, but rather formed a separate family of states. Aperiodic oscillations were also observed. We are able to construct one-humped, one-dimensional maps from data in the time series of these aperiodic oscillations which implies that their origin is deterministic chaos. The results of our measurements on the various types of behavior within the oscillatory region are presented in this section.

A. Period doubling bifurcations, chaos, and one-dimensional maps

We now describe a ubiquitous set of dynamical behaviors observed in the copper–phosphoric acid systems that was achieved at several values of the rotation rate by slowly varying the applied potential. Measured waveforms of the current for one such value of the rotation rate are shown in Fig. 6. Beginning an experiment with the system in the asymptotic oscillatory state corresponding to the waveform shown in Fig. 6(a), a period-one state, and slowly decreasing the potential, a critical value was reached at which point the period doubled, signaling the transition to a different oscillatory state, a period-two state. At values of the potential less

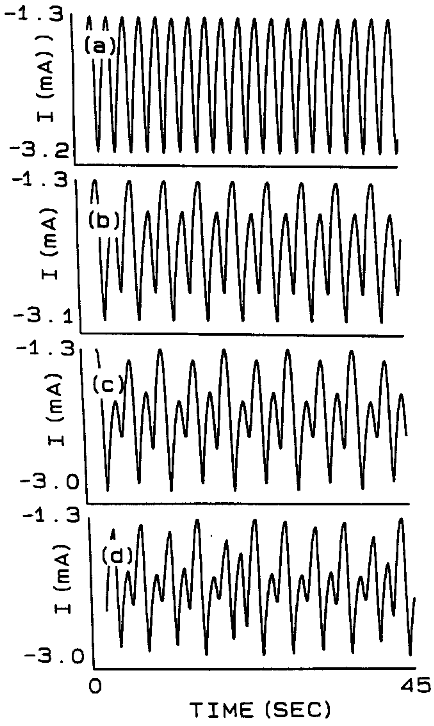

FIG. 6. A subharmonic sequence. Measured current is plotted as a function of time. Rotation speed = 4600 rpm. (a) Primary, period-one oscillations; $V_0 = 448.0$ mV; (b) period-two oscillations, $V_0 = 446.0$ mV; (c) period-four oscillations, $V_0 = 445.2$ mV (d) an aperiodic time series, $V_0 = 445.0$ mV.

than the critical value, the measured time series for the period-two state consists of alternating peaks of two different amplitudes; see Fig. 6(b). Decreasing the potential further led to a second bifurcation in which the period doubled again and the system made a transition to another oscillatory state, a period-four state.

These observations are consistent with those expected when a system is moved through the first two bifurcations of an infinite sequence of period doubling bifurcations. Nonlinear dynamical theory predicts that the distance in parameter space between consecutive bifurcations decreases geometrically in the direction of a limit point. Consequently, asymptotic states of higher order period are difficult to observe. The highest order, asymptotic, periodic state that was recorded in our experiments is a period-four state, Fig. 6(c).[27]

Theory also predicts that chaotic states exist just beyond the limit point of the sequence of period doubling bifurcations. Several measured waveforms are consistent with those of chaotic oscillations since they appear aperiodic and random in the sense that even with the knowledge of the past history of the time series it is impossible to predict its future. One example of a measured waveform that corresponds to an aperiodic oscillation with this random property is shown in Fig. 6(d). Aperiodic oscillations were observed at values of the potential that are slightly less than the value used to obtain the period-four oscillations in Fig. 6(c).

We have also constructed three-dimensional phase portraits using the time-delay method. Trajectories corresponding to the period-two, period-four, and aperiodic oscillations are shown in Fig. 7 projected into the $[I(t+T), I(t)]$ plane. Aperiodic trajectories in the three-dimensional space $[I(t), I(t+T), I(t+2T)]$ were found to cross the plane, $I(t+2T) = -1.40$ mA, at points that approximately formed a one-dimensional rectilinear curve. Plotting $I(n+1)$, the value of $I(t)$ at the $(n+1)$th intersection against $I(n)$, the value of $I(t)$ at the nth intersection, produces a one-dimensional mapping. Two examples of such mappings are represented in Fig. 8. A one-dimensional

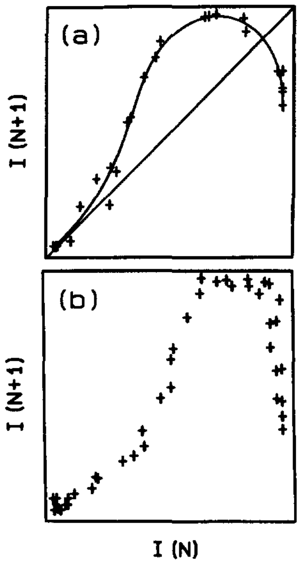

FIG. 8. One-dimensional maps (a) $V_0 = 445.1$ mV, (b) $V_0 = 445.0$ mV, rotation rate = 4600 rpm. The maps demonstrate that the apparent random behavior is deterministic: for any $I(n)$, the maps give $I(n+l)$. The presence of the extremum implies that the deterministic dynamics is chaos (Refs. 13 and 14).

curve, that defines a function $F(I)$, can be drawn through the iterates of the maps and so the mappings can be represented by a difference equation, $I(n+1) = F[I(n)]$. The construction of one-dimensional maps from "asymptotic" "trajectories" for which $F(I)$ possesses an extremum implies that the underlying dynamics are chaotic.

The location in parameter space at which subharmonic and aperiodic oscillations were observed is shown in Fig. 9. Notice that in this system chaos can also be approached through period doubling bifurcations by increasing the potential (see Fig. 9). We also show the location of parameter values in this phase diagram where mixed-mode oscillations (MMO) were found. The behavior of these states is discussed next.

B. Mixed-mode oscillations

In the part of the parameter plane denoted by MMO, Fig. 9, we observed mixed mode oscillations similar to those

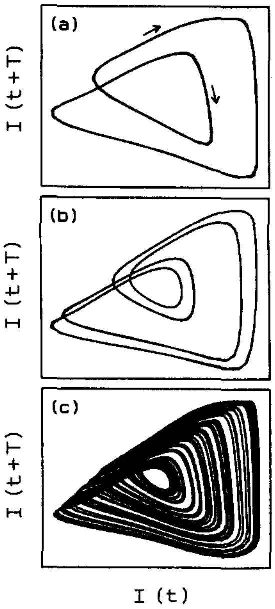

FIG. 7. Phase trajectories constructed from the time series data, Fig. 6, shown projected into the $[I(t), I(t+T)]$ plane; $T = 0.73$ s. (a) A period-two orbit; (b) a period-four orbit; (c) an aperiodic orbit. Parameter values are the same as Fig. 6.

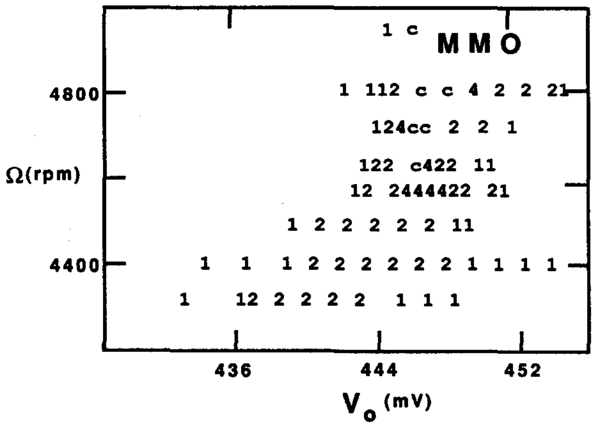

FIG. 9. Phase diagram [rotation speed (Ω) vs potential set for the working electrode (V_0)] showing the location of different oscillatory states; Temperature = -17.5 °C. Notation: 1 = period-one state; 2 = period-two state; 4 = period-four state; C = chaotic state; MMO = mixed-mode oscillations.

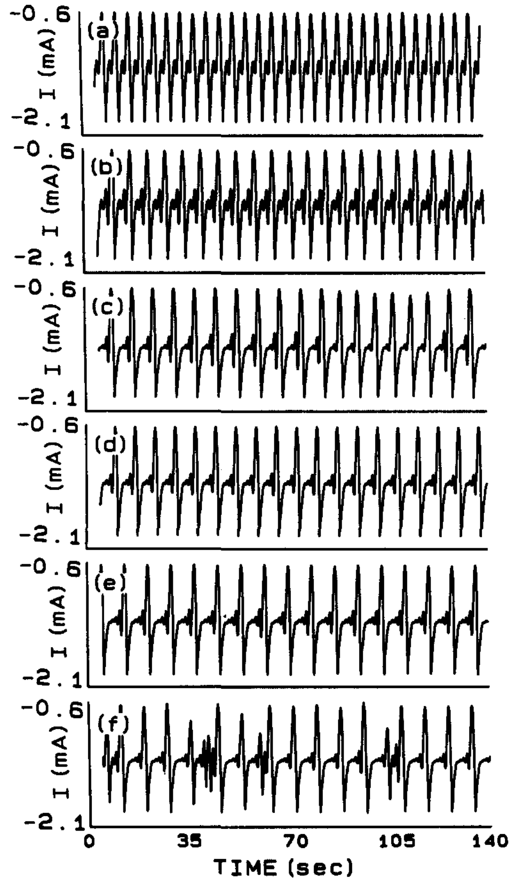

FIG. 10. Measured waveforms that correspond to mixed-mode oscillations. Current is plotted as a function of time. Temperature = − 24.5 °C. Rotation speed = 5500 rpm. (a) P_1^1, $V_0 = 405.5$ mV; (b) P_1^2, $V_0 = 404.75$ mV; (c) $C_1^{2,3}$, $V_0 = 404.5$ mV; (d) P_1^3, $V_0 = 404.0$ mV; (e) P_1^4, $V_0 = 403.75$ mV; (f) C^n, $V_0 = 403.35$ mV.

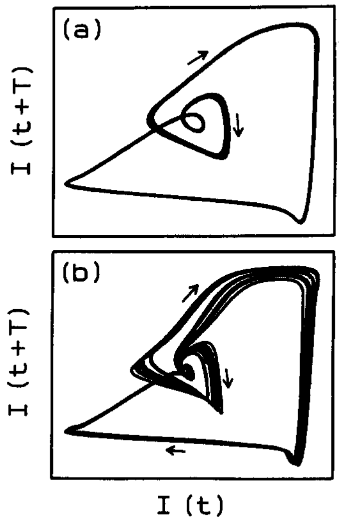

FIG. 11. (a) Phase trajectory shown projected into the $[I(t), I(t) + T)]$ plane constructed from the time series in Fig. 10(b). $T = 0.73$. (b) The same as (a) but constructed from the time series in Fig. 10(c).

found near the high potential boundary in Fig. 2 and discussed in Sec. III. The asymptotic behavior was found to change rapidly with respect to variation of either the applied potential or the rotation rate. Consequently, a pattern in the bifurcation structure could not be resolved. These behaviors, however, extended to lower temperatures. At the temperature − 24.5 °C, we are able to identify the following sequence:

$$P_1^1 \to C_1^{1,2} \to P_1^2 \to C_1^{2,3} \to P_1^3 \to C_1^{3,4} \to P_1^4 \to \cdots C_1^n\ , \quad (4.1)$$

where we have used the notation found in Swinney and Roux[13(a)]: P and C denote periodic and chaotic dynamics, respectively. In the case of periodic behavior, the subscripts refer to the number of large amplitude oscillations in a period, and the superscript refer to the number of seqential small amplitude oscillations. The chaotic oscillations appear as a random combination of the periodic oscillations that immediately precede and follow the chaotic state in the sequence, Eq. (4.1).[28]

Some of the measured waveforms corresponding to the different states in the sequence, Eq. (4.1), are shown in Fig. 10. Two phase portraits, one constructed form the periodic-time series in Fig. 10(b) and the other constructed from the aperiodic time series in Fig. 10(c), are shown in Fig. 11. The aperiodic orbit first moves around the inside and then on the outside of the smallest loop, Fig. 11(b). The orbit then appears to randomly choose between going immediately to the outside loop or first traveling around the intermediate size loop. These phase portraits suggest that a mechanism exists that reinjects an orbit into the vicinity of a fixed point located at the center of the small loops. However, we cannot provide evidence that the fixed point is located there.

Mixed mode oscillations were found over a wide range of parameter values in the copper–phosphoric acid system. The sequence, Eq. (4.1), as well as the qualitative features of the corresponding waveforms, Fig. 10, have been observed in the Belousov–Zhabotinskii reaction.[13–15]

V. AN ADDITIONAL OBSERVATION AND DISCUSSION

The achievement of a theoretical description of the dissolution of copper in phosphoric acid will require a formulation of the basic steps in the electrokinetic mechanism. Several mechanisms postulate a direct transformation from copper(0) to copper(II).[11,12] Several times we have observed fine particles, which had the same appearance as those produced in the polishing of the copper disk, in a spiral pattern on the outer Teflon portion of the disk. The formation of copper implies a more complex mechanism that probably contains the reaction of disproportionality, the transformation from copper(I) to copper(0) and copper(II).[29] As a caution, we note that our observations of copper on the outer portion of the disk were made only when noticeable changes occurred in the measured current and were accompanied with a visible surface deformation in the disk (≈ 0.2 mm in diameter and ≈ 0.1 mm in depth).

Our experimental study of the dissolution of copper in phosphoric acid shows that a large number of dynamical states exist in this system. These states, which include mixed-mode oscillations, subharmonics, and chaotic oscillations, were characterized and distinguished through the construction of waveforms, phase portraits, and mappings. We were able to locate the position of Hopf bifurcations and sequences of period doubling bifurcations in phase diagrams. The characterization of states and phase diagrams provide tests for theoretical descriptions of the electrochemical processes that accompany the dissolution of copper from a rotating disk in phosphoric acid. We are not aware of any theory that is capable of predicting our experimental results.

Near the completion of this work we became aware of other studies of nonlinear behavior in other electrochemical systems. Diem and Hudson[30] have shown that hyperchaos occurs in a system consisting of sulfuric acid and an iron rotating disk. Bassett and Hudson[31] have characterized several types of behavior in the dissolution of copper in acidic chloride media, including both chaotic and quasiperiodic states. These results, as well as the results presented in this paper, indicate that electrochemical systems may provide experimental paradigms for the study of nonlinear dynamical behavior.

ACKNOWLEDGMENT

This research was supported by The Robert A. Welch Foundation-Grant No. N-1096.

[1]Some examples are: J. H. Bartlett, Trans. Electrochem. Soc. **87**, 521 (1945); K. F. Bonhoeffer and W. Jena, Z. Elektrochem. **55**, 151 (1951); D. Gilroy and B. E. Conway, J. Phys. Chem. **69**, 1259 (1965); M. L. B. Rao, J. Electrochem. Soc. **114**, 665 (1967); U. F. Franck, Faraday Symp. Chem. Soc. **9**, 137 (1974); P. Poncet, M. Braizaz, B. Pointer, J. Rousseau, and N. Muhlstein, J. Chim. Phys. **75**, 287 (1978); R. De Levie, J. Electroanal. Chem. **25**, 257 (1970).

[2]P. Russell and J. Newman, J. Electrochem. Soc. **133**, 2093 (1986).

[3]An observation of a period doubling bifurcation and the suggestion of deterministic chaotic oscillations are found in: A. L. Kawcznski, M. Przasnyski, and B. Baranowski, J. Electroanal. Chem. **179**, 285 (1984).

[4]S. H. Glarum and J. H. Marshall, J. Electrochem. Soc. **132**, 2872, 2878 (1985).

[5]H. P. Lee, K. Nobe, and A. J. Pearlstein J. Electrochem. Soc. **132**, 1031 (1985).

[6]A. J. Pearlstein, H. P. Lee, and K. Nobe, J. Electrochem. Soc. **132**, 2159 (1985).

[7]H. Degn, Trans. Faraday Soc. **64**, 1348 (1968).

[8]J. Keizer, P. K. Rock, and S.-W. Lin, J. Am. Chem. Soc. **101**, 5637 (1979); J. Keizer and D. Scherson, J. Phys. Chem. **84**, 2025 (1980).

[9]J. B. Talbot, R. A. Oriani, and M. J. DiCarlo, J. Electrochem. Soc. **132**, 1545 (1985).

[10]C. G. Law and J. Newman, J. Electrochem. Soc. **126**, 2150 (1979); **133**, 37 (1986).

[11]V. A. Dmitriev and E. V. Rzhevskaya, Russ. J. Phys. Chem. **35**, 425 (1961).

[12]E. C. Williams and M. A. Barrett, J. Electrochem. Soc. **103**, 363 (1956); K. Kojima and C. W. Tobias, *ibid.* **120**, 1026 (1973).

[13]H. L. Swinney and J. C. Roux, in *Nonequilibrium Dynamics in Chemical Systems*, edited by C. Vidal and A. Pacault (Springer, New York, 1984), p. 124; F. Argoul, A. Arneodo, P. Richetti, J. C. Roux, and H. L. Swinney, Acc. Chem. Res. **20**, 436 (1987).

[14]R. H. Simoyi, A. Wolf, and H. L. Swinney, Phys. Rev. Lett. **49**, 245 (1981); J. C. Roux, R. H. Simoyi, and H. L. Swinney, Physica D **8** 257 (1983).

[15]J. L. Hudson, M. Hart, and D. Marinko, J. Chem. Phys. **71**, 1601 (1979); J. L. Hudson and J. C. Mankin, *ibid.* **74**, 6171 (1981).

[16]K. G. Coffman, W. D. McCormick, and H. L. Swinney, Phys. Rev. Lett. **56**, 999 (1986); K. G. Coffman, W. D. McCormick, Z. Noszticzius, R. H. Simoyi, and H. L. Swinney, J. Chem. Phys. **86**, 119 (1986).

[17]J. Maselko and H. L. Swinney, Phys. Lett. A **119**, 403 (1987); J. Maselko and H. L. Swinney, J. Chem. Phys. **85**, 6430 (1987).

[18]L. P. Sil'nikov, Math. USSR S. **10**, 91 (1970).

[19]A. Arneodo, P. Coullet, and C. Tresser, J. Stat. Phys. **27**, 171 (1982); P. Glendinning and C. Sparrow, *ibid.* **35** (1984); P. Gaspard, R. Kapral, and G. Nicolis, *ibid.* **35**, 697 (1984).

[20]A. J. Lichtenberg and M. A. Lieberman, *Regular and Stochastic Motion*, Appl. Math. Sci. Vol. 38 (Springer, New York, 1983), Chap. 7.

[21]A. J. Bard and L. R. Faulkner, *Electrochemical Methods Fundamentals and Applications* (Wiley, New York, 1980), (a) Sect. 8.3; (b) Sect. 1.3.4.

[22]J. Marsden and N. McCraken *The Hopf Bifurcation and Its Applications*, Appl. Math. Sci. Vol. 19 (Springer, New York, 1976).

[23]F. Argoul, A. Arneodo, P. Richetti, and J. C. Roux, J. Chem. Phys. **86**, 3325 (1987).

[24]Inverted Hopf Bifurcations (subcritical Hopf) were observed in nonlinear chemical reactions earlier; see, e.g., P. DeKepper and J. Boissonade, J. Chem. Phys. **75**, 189 (1981).

[25]P. Richetti and A. Arneodo, Phys. Lett. A **109**, 359 (1985); A. Arneodo, P. H. Coullet, E. A. Spiegel, and C. Tresser, Physica D **14**, 327 (1985).

[26]Either a transition from the small amplitude periodic oscillations to quasiperiodic behavior via a second Hopf Bifurcation or the presence of a bistability are also expected to occur along the line A–B; see Ref. 25. We did not observe these phenomena.

[27]We observed what appeared to be period-eight and period-sixteen states for approximately 60 oscillations, but then the system settled down into either a period-four or an aperiodic state.

[28]Periodic-chaotic sequences, such as that given in Eq. (4.1), and purely periodic sequences of mixed-mode oscillations have been observed in the same system but under different constraints, see Ref. 13. A possible explanation for the purely periodic sequence in terms of a limit of a circle map is given by: D. Barkley, Phys. Rev. Lett. (submitted).

[29]G. Kortum, *Treatise on Electrochemistry* (Elsevier, Amsterdam, 1965), pp. 504,505.

[30]C. B. Diem and J. L. Hudson, AIChE J. **33**, 218 (1987).

[31]M. R. Bassett and J. L. Hudson, Chem. Eng. Comm. (in press); M. R. Bassett and J. L. Hudson, *Homoclinic Chaos, Quasiperiodicity, Noodal Maps and Other Phenomena in Electrochemical Reactions*, Proceedings Spatial Inhomogenities and Transient Behavior, Bruxelles, Belgium, 1987.